Air Quality, Atmosphere & Health
https://doi.org/10.1007/s11869-024-01571-w

Atmospheric deposition studies of microplastics in Central Germany

Sarmite Kernchen[1,2] · Holger Schmalz[3,4] · Martin G. J. Löder[2] · Christoph Georgi[5] · Andrej Einhorn[1] · Andreas Greiner[3,4] · Anke C. Nölscher[1] · Christian Laforsch[2] · Andreas Held[5]

Received: 18 October 2023 / Accepted: 8 April 2024

Abstract
Emission of microplastics (MP) to the atmosphere, airborne transport, and subsequent deposition are now recognized. However, the temporal and spatial resolution of data on MP pollution and knowledge of their atmospheric behaviour and fate is still very limited. Hence, we investigated MP wet and dry deposition in Central Germany and examined the role of weather conditions on MP contamination levels. Monthly samples of dry and wet deposition were taken over an eight-month period (05/2019-12/2019) and analysed by micro-Fourier-Transform Infrared spectroscopy (µFTIR) down to 11 µm particle size and one dry deposition sample was subjected to Raman analysis to determine plastic particles down to a size of 0.5 µm. MP in a size range from 11 µm to 130 µm were detected in all wet deposition samples and in 4 out of 8 dry deposition samples by µFTIR. Polypropylene particles were found most frequently and accounted for 62% and 54% of all particles in wet and dry deposition samples, respectively. Over the eight-month period, wet deposition of MP slightly dominated at the study site and comprised 59% of the total MP deposition. The MP mean total (wet + dry) deposition flux (DF) was 17 ± 14 MP m^{-2} day^{-1}. Extensive Raman analyses of an exemplary dry deposition sample revealed additional plastic particles in the extended size range from 1 to 10 µm resulting in a deposition flux of 207 MP m^{-2} day^{-1}. Our results suggest that MP analysis by µFTIR down to 11 µm may underestimate DF at least by an order of magnitude. More comprehensive studies on submicron plastics and nanoplastics are needed to fully assess air pollution by plastic particles.

Keywords Plastic pollution · Wet, dry and total deposition of microplastics · µFTIR · Raman spectroscopy

Introduction

Air pollution is one of the biggest threats to human health, causing millions of deaths worldwide every year (Manisalidis et al. 2020). Despite efforts to reduce air pollution, the majority of the world's population continues to be exposed to increasing levels of air pollution substantially above WHO Air Quality Guidelines (Shaddick et al. 2020). Recently, small plastic particles were determined as a widespread airborne anthropogenic pollutant, whose distribution in the atmosphere and deposition can now be expected all over the globe (Zhang et al. 2019; Enyoh et al. 2019; Huang et al. 2020; Prata 2018). These pollutants may have been polluting the atmosphere since the plastic industry began but are only now being addressed. Studies show a variation over several orders of magnitude of airborne microplastic (MP, particles with the largest dimension from 1 µm to < 1000 µm (Hartmann et al. 2019) concentrations and deposition fluxes (DF). Observed MP concentrations range from 0.01 m^{-3} in the remote marine atmosphere (Trainic et al. 2020) to 2502 m^{-3} in urban road-side London (UK) (Levermore et al. 2020) and DF between 10 ± 8 m^{-2} day^{-1} in the urbanised coastal zone of the Gulf of Gdansk (Poland) (Szewc et al. 2021) to 771 ± 167 m^{-2} day^{-1} in central London (UK) (Wright et al. 2020). Further, the atmosphere can significantly contribute

✉ Sarmite Kernchen
Sarmite.Kernchen@uni-bayreuth.de

1 Chair of Atmospheric Chemistry, BayCEER, University of Bayreuth, 95440 Bayreuth, Germany

2 Chair of Animal Ecology I, BayCEER, University of Bayreuth, 95440 Bayreuth, Germany

3 Chair of Macromolecular Chemistry II, University of Bayreuth, 95440 Bayreuth, Germany

4 Keylab Synthesis and Molecular Characterization, Bavarian Polymer Institute, University of Bayreuth, 95440 Bayreuth, Germany

5 Chair of Environmental Chemistry and Air Research, Technische Universität Berlin, 10623 Berlin, Germany

to the plastic pollution of terrestrial and aquatic systems through airborne transport over long distances up to several thousands of kilometres far from their sources (Bergmann et al. 2019; Trainic et al. 2020; González-Pleiter et al. 2021). Suspended in the air, MP may have direct radiative effects that influence Earth's climate by absorbing and scattering radiation. These effects were assessed as minor but with a tendency to increase if the plastic production and waste management practices will remain unchanged (Revell et al. 2021). MP deposited into marine waters, soils, or plants can cause substantial damage and stress to the environment and human health due to their uptake and accumulation in food chains (Anbumani and Kakkar 2018; Fang et al. 2022). Direct effects are also suspected, as MP can enter the human body through the respiratory tract. Studies in the German Weser River catchment revealed that a human may breathe in on average 500 MP particles per day (Kernchen et al. 2021), which is probably underestimated since only particles down to 4 µm were analysed. In fact, MP particles have been detected in human lung tissue collected during autopsies (Amato-Lourenço et al. 2021) and thoracic surgery (Jenner et al. 2022a). In addition to this, tests on human alveolar cells showed that airborne polystyrene MP may have toxicologic consequences on human health (Goodman et al. 2021). Despite these public concerns, atmospheric MP are relatively sparsely studied, and more reliable data on MP levels and behaviour in the atmosphere are needed to better assess these impacts.

Unfortunately, most of the current analytical techniques used for MP identification are limited with respect to particle size (Zhang et al. 2020). Detecting plastic particles in the size range most relevant for inhalation (aerodynamic diameter < 10 µm) is time-consuming and expensive (Zhang et al. 2019). Therefore, the vast majority of studies focusing on airborne MP use techniques with an analytical threshold of geometric diameters > 10 µm. Only a few methods are suitable for the detection of individual polymer fragments in the lower µm-range (1 to 10 µm) and, submicron range (0.1 to < 1 µm), and ultrafine or nano range (≤ 0.1 µm), and up to date lack the routine methodology (Schwaferts et al. 2019). Currently, by using Raman imaging the smallest MP particles measured in a real sample were down to 100 nm in size (Sobhani et al. 2020b). FTIR and Raman spectroscopy are the most frequently applied methods in MP studies, and it has been suggested to use them in tandem for complete and reliable chemical characterization of MP (Käppler et al. 2016). Even though both methods are vibrational spectroscopic methods, they complement each other and may provide different numbers and polymer types of detectable MP.

Hence, to complement our knowledge on MP contamination levels in the atmosphere, and to investigate MP dry and wet deposition, we studied the temporal variation in MP deposition and evaluated the relative efficiency of MP (> 11 µm) dry and wet removal in Central Germany. Specifically, the following objectives were pursued: (i) to collect monthly wet and dry deposition samples over the time-period of eight months (05/2019-12/2019); (ii) to count and to determine the type, shape, size, and the colour of the plastic particles by micro-Fourier-Transform Infrared spectroscopy (µFTIR) down to 11 µm in size; (iii) to investigate the relationships between MP deposition fluxes/MP concentrations in precipitation and meteorological parameters, the local wind fields, and population-weighted air mass back trajectories. In addition to this, one exemplary dry deposition sample was studied by Raman spectroscopy (iv) to detect MP particles smaller than 11 µm (i.e., below the detection limit of µFTIR).

Materials and methods

Sampling site and meteorological conditions during sampling

The study site (latitude 51.32476 °N, longitude 9.52471 °E) was located in an urban area in Central Germany ~ 3 km northeast (NE) of the city centre of Kassel. The city had a population of 202,137 in 2019 and a population density of 1,900 people km^{-2}. It represents an average central German city with industry and rural areas in the neighbourhood. Similar MP pollution is to be expected in many German cities and thus represents pollution in a larger area. The average temperature during the sampling period was 13.8 °C, with a total precipitation of 408 L m^{-2}. Meteorological data for the sample collection period were retrieved from the wastewater treatment plant *KasselWasser* and the nearest weather station *Kassel-Mitte* (Hessisches Landesamt für Naturschutz, Umwelt und Geologie). The monthly precipitation highly varied in the sampling period. The highest monthly precipitation sum was 93 L m^{-2} in May and lowest was 32 L m^{-2} in September. The measured rainfall intensity ranged from 0.28 to 0.88 mm h^{-1}. In the sampling period, two wind directions were dominant, south-southwest (SSW) and NE, respectively. The average wind speed over the sampling period was 1.8 m s^{-1} corresponding to a light breeze and calm periods (see Fig. 1 and Online Resource ESM_1 for details of daily precipitation during the sampling period and other meteorological parameters).

Collection of dry and wet atmospheric deposition

Wet and dry atmospheric deposition samples were collected for intervals of calendar months in 2019 starting with May and ending with December sample. For sample

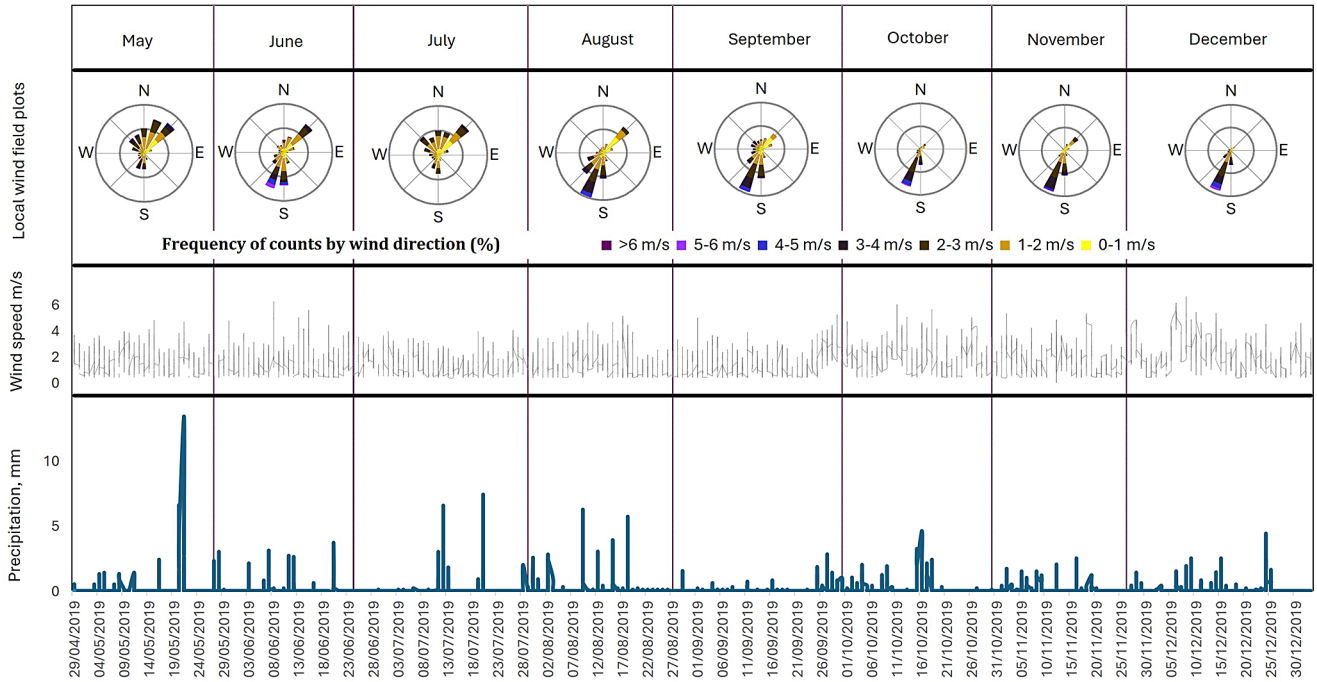

Fig. 1 Daily precipitation, wind speed and local wind field plots at the sampling site in Kassel over monthly wet and dry deposition collection periods (indicated by vertical lines)

collection, a custom-made automatic collector (University of Bayreuth (UBT), length x width x height = 0.6 m x 0.3 m x 1 m) with two separate units was built and installed at the sampling site in Kassel (see Online Resource ESM_1). The wet deposition sample collection unit consisted of a collection funnel, a stainless-steel filtration device (Whatman MV050 series, 500 mL, appropriate for filter diameters of 47/50 mm) and a stainless-steel lid. Controlled by a rain sensor (Kemo M152, 12 V, Germany), the collection funnel was opened during rain or snow, and the lid closed during dry periods. Wet deposition samples were in-situ filtered through pre-cleaned stainless-steel filters (⌀ = 47 mm, pore size 10 µm, Wolftechnik Filtersysteme GmbH & Co, Germany). The dry deposition sampling unit was a simplified modification based on the Sigma-2 passive sampler for collecting settling particles (VDI2119 2013; Dietze et al. 2006; Waza et al. 2019). Briefly, the sampler consists of a cylindrical stainless-steel sedimentation tube with diameter of 101 mm, which is covered with a stainless-steel cap (150 mm x 70 mm) so that it was sheltered from rain from above, but horizontal wind drafts can carry particles through the 23 mm slit on the side of the sampler between the tube and the lid. Due to gravitation, passively entered particles settle down to the collection surface. Particles were collected on pre-cleaned circular stainless-steel plates (custom-made at UBT, ⌀ = 104 mm x 1 mm) to allow particle rinsing, sub-sampling, and re-filtering (see Sample pre-treatment).

In total, 8 monthly wet and dry deposition samples were collected from May 2019 to December 2019. Filters and plates for collection of wet and dry deposition were changed on the same days. Sampling started when the filters/plates were inserted into the sampling units and ended when they were removed from the collector. This time refers to the sampling time during which the sampling units were opened or closed for sampling, depending on the weather conditions. The average collection time was 30 days. Three wet deposition and three dry deposition blank samples were taken in the same manner as field samples omitting the collection step. After collection, the stainless-steel filters and plates were placed in pre-cleaned Petri dishes, wrapped in aluminium foil and stored in a refrigerator at 4 ºC until they were brought to the laboratory for further processing. This minimised the growth of algae and mould, which otherwise could interfere the detection of MP. 22 different types of plastic that we can detect are not degraded under these conditions.

Contamination control

To prevent contamination, the samples were handled under a laminar flow box whenever possible (Laminar Flow Box FBS, Spetec GmbH). Furthermore, the laboratory was equipped with an air purifier (DustBox with

HEPA H14 filter, Möcklinghoff Lufttechnik GmbH) to reduce airborne contamination. Special care was taken to keep all the units and solutions which came into contact with the sample clean from detectable plastic particles. Rinsing solutions were filtered through a 0.2 µm membrane filter (47 mm, cellulose acetate, Whatman, Japan) before use. All glassware, sampling units, tweezers, stainless-steel filters, Petri dishes, and all components of the vacuum filtration devices were thoroughly rinsed with pre-filtered MilliQ water, followed by rinsing with pre-filtered 35% ethanol, and repeatedly washed with pre-filtered MilliQ water. All pre-cleaned units were stored covered with non-plastic lids or wrapped in aluminium foil to minimize contamination from laboratory air. Stainless-steel filters were placed in the ultrasound bath and sonicated for 2 min before a standardized rinsing process. Solutions were stored either in glass bottles or in stainless-steel or Teflon spray bottles. The use of plastic tools, containers, and other laboratory equipment was avoided. The laboratory is equipped exclusively for MP analyses and no external tasks are allowed. Cotton laboratory coats were always worn during the procedures to prevent any contamination of synthetic fibres from clothing.

Sample pre-treatment

Particles in wet deposition samples which were in-situ filtered on stainless-steel filters and Petri dishes were rinsed thoroughly in separate glass beakers with pre-filtered water. The particles were re-filtered through the same stainless-steel filter using a stainless-steel filtration device (Sartorius 16828, filter holder with 3 × 500 mL manifolds) so that the particles were evenly distributed on the filter and halved using split pliers (custom-made at UBT, suitable for filters ⌀ = 47 mm, enables half the particulate load on the filter to be rinsed off). The rinsed particles were resuspended on two to four Anodisc filter(s) (pore size 0.2 µm, ⌀ = 25 mm, Anodisc25, Whatman, Germany) depending on particle load in a subsample using a custom-made (UBT) filtration device consisting of a stainless-steel filter manifold (⌀ = 30 mm) with glass frit (⌀ = 9 mm) and glass funnel (V = 5 mL). The dry deposited aerosol on stainless-steel circles was rinsed off with prefiltered MilliQ water and filtered through membrane filters (0.2 µm, ⌀ = 47 mm, Isopore, GTTP, Merck Millipore Ltd., Ireland). One half of the particulate matter was rinsed off by using split pliers and resuspended onto one to four Anodisc filters. The other half of the particles on the filters were stored in the fridge as a backup sample. Thus, subsamples corresponding to 50% of each wet and dry deposition sample were rinsed off and resuspended on Anodisc filters.

Background contamination

Wet and dry deposition blanks were subjected to all sample treatments as for the field samples to assess contamination that may occur during sample processing. Four out of six wet and dry deposition field blanks were free from MP and the remaining blanks contained individual polystyrene (PS) fragments (length, width: 60 µm, 41 µm and 139 µm, 81 µm). Thus, the blank samples contained a mean value of 0.33 ± 0.58 PS particles per wet and dry deposition samples which result in limit of detection (LOD) of 2.1 (mean + 3 x standard deviation (SD) and limit of quantification (LOQ) of 6.1 (mean + 10 × SD) (Schymanski et al. 2021; Horton et al. 2021). Since laboratory contamination is attributable to one polymer type only, the results for all other polymer types of the wet and dry deposition samples were considered as valid (Schymanski et al. 2021). Only one dry deposition sample and two wet deposition samples contained single PS particles similar in size to the MP fraction in the blank samples. The LOD for PS particles is higher than particle number in a sample, therefore, PS polymer type was excluded from all wet and dry deposition series. Since no other than PS particles were present in the blank samples, the results are presented without prior subtraction of blank values.

µFTIR analysis

The samples on the Anodisc filters were measured with focal plane array (FPA) based micro-Fourier-Transform Infrared spectroscopy (µFTIR) with the IR microscope Hyperion 3000 (Bruker Inc., Billerica, USA) coupled to a Tensor 27 spectrometer (Bruker Optik GmbH, Ettlingen, Germany). The microscope was equipped with a 3.5 x IR objective and liquid nitrogen cooled FPA detector operating with 64 × 64 pixels for chemical imaging described by Löder et al. (Löder et al. 2015) resulting in a pixel size of 11 µm. MP particles (> 11 µm) were analyzed in transmission mode on a CaF_2 transmission window (⌀ = 13 mm, d = 2 mm). Samples were scanned in the wavenumber range from 1250 to 3600 cm^{-1} with a spectral resolution of 8 cm^{-1} and an accumulation of 36 scans. The background was measured for each filter separately in the area of the filter where no particles were observed. The entire particle-loaded filter area (~ 10 × 10 mm^2) was scanned. Thus, an infrared map consisting of around 1 million individual spectra was acquired. Particle identification and quantification was done using the software OPUS 7.5 (Bruker Optik GmbH) and ImageLab in combination with a commercial, custom-made software tool *Purency* based on random

decision forest classifiers as described by Hufnagl et al. (Hufnagl et al. 2019, 2021). This commercially available software tool automatically searches for IR spectra of the 22 most common synthetic polymers. The location, major and minor dimensions of the identified MP particles, colour, and polymer assignment were recorded. All FTIR spectra were compared with reference spectra from a database and only well-fitted spectra were assigned as MP. Each automatically identified microplastic particle was manually double-checked against reference spectra according to a four-eye principle by experienced personal for quality assurance.

Raman analysis

For Raman measurements a WITec alpha 300 RA + imaging system (WITec GmbH, Ulm, Germany), equipped with a UHTS 300 spectrometer and a back-illuminated Andor Newton 970 EMCCD camera was employed. An excitation wavelength of $\lambda = 532$ nm and a 50x objective (Zeiss EC Epiplan-Neofluoar HD, NA = 0.8) together with the WITec suite FIVE 5.3 software package were used for all measurements. The WITec ParticleScout particle analysing tool together with the WITec TrueMatch data base managing software (ST Japan, SPECARB and in-house polymer data bases) were utilized for MP detection and identification on the Anodisc filter sample.

Five randomly selected areas on the filter were chosen for Raman investigations. An optical stitching image was taken over an area of 3×3 mm^2 and was scanned, employing the WITec ParticleScout particle analysing software. In this area, Raman spectra were acquired automatically followed by screening of the obtained Raman spectra with the TrueMatch database managing software. In addition, the identified MP were measured manually using an integration time of 0.5 s and 50 accumulations (laser power: 5 mW). At four selected positions, large area Raman mapping was performed in order to probe for particles with sizes well below 5 µm employing following conditions: (i) scan area 500×500 µm^2, integration time 0.8 s, step size 2 µm pixel^{-1}, laser power 10 mW; (ii) scan area 100×100 µm^2, integration time 0.6 s, step size 0.5 µm pixel^{-1}, laser power: 8 mW. For all large area scans the focus was set close to the filter surface in order to be able to probe the presence of small particles. The component distributions in large area scans were determined using the True Component Analysis option in the WITec Project FIVE 5.3 software. All spectra were subjected to a cosmic ray removal routine and baseline correction.

Calculations & statistical analysis

MP wet and dry DF were calculated according to Kernchen et al. (2021). Briefly, MP wet and dry number DF were calculated from the count of plastic particles in a sample divided by the exposed surface area of collection (1.08×10^{-2} m^2 for wet deposition samples and 8.01×10^{-3} m^2 for dry deposition samples) and duration of sampling (days) (Eq. 1).

$$DF_{w,d} = \frac{\chi\gamma}{at} \quad \text{(Eq. 1)}$$

where $DF_{w,\,d}$ – (wet and dry deposition flux, MP m^{-2} day^{-1}); χ –count of MP in a subsample; γ – subsample size; a – exposed surface area of the collector; t –duration of sampling.

Total deposition flux (DF_t) was calculated by summing wet and dry DF (Eq. 2).

$$DF_t = DF_w + DF_d \quad \text{(Eq. 2)}$$

MP concentrations in precipitation (C_{MP}, MP L^{-1}) were calculated by dividing MP count in a sample to collected precipitation volume (V) and multiplying to total precipitation amount per m^2 over each sampling period (P) (Eq. 3).

$$C_{MP} = \frac{\chi\gamma}{VP} \quad \text{(Eq. 3)}$$

For calculations of dry deposition velocities please refer to Online Resource ESM_1. 24-hour air mass back trajectories were calculated using the air parcel trajectory model HYSPLIT4 (Stein et al.2015) and NCEP/NCAR reanalysis data (Kalnay et al. 1996). Trajectory-averaged population densities were determined for each sampling period according to the following procedure: (i) For each day of the sampling period, eight 24-hour back trajectories were calculated arriving at 00:00, 03:00, 06:00, 09:00, 12:00, 15:00, 18:00, and 21:00 at 100 m above ground level at the study site in Kassel. (ii) For each 24-hour back trajectory, the trajectory-averaged population density was calculated from the 24 population densities determined hourly along the air mass trajectory. Every hour, the population density (number of people per square kilometre) at the air parcel position was taken from the German Census data 2011 on a 1 km x 1 km grid, and averaged. Less than 5% of the air parcel positions along the 24-hour back trajectories were outside of Germany, and ignored. (iii) For the entire sampling period, all trajectory-averaged population densities of all sampling days were averaged. Relationships between DF and meteorological variables were estimated by means of Spearman rank correlations. Two means were tested using student's

significant *t*-test with a significance level set at 0.05. All statistical analyses were performed with the freely available statistical computing software Past (v.4.03).

Results

Characterization of MP particles (> 11 µm) detected in wet and dry deposition samples by µFTIR

In the studied time period, MP particles in size > 11 µm were detected in all monthly collected wet deposition samples and in 4 out of 8 dry deposition samples (Table 1). In total, 8 particles found in dry deposition samples and 13 particles in wet deposition samples were assigned to common synthetic polymers and referred to pollution in deposition samples. Overall, the mean of 1.63 ± 0.92 MP per wet deposition sample and 0.88 ± 1.1 MP per dry deposition sample were identified by µFTIR.

The average MP particle size in wet deposition samples (50 ± 37 µm, mean ± SD) was slightly larger than the average MP particle size in dry deposition samples (45 ± 21 µm, mean ± SD) but not significantly different ($p > 0.05$). MP particles < 100 µm were observed both in dry and wet deposition samples, whereas particles larger than 100 µm were identified in wet deposition samples only. Calculated dry deposition velocities ranged from 0.05 to 0.2 m s^{-1}. Eighteen of the detected MP particles were in the shape of fragments, while three were one pixel in size and their exact shape could not be determined. In total, particles made of five different polymer types were found in wet and dry deposition samples by µFTIR. Twelve of the seventeen MP particles were made of polypropylene (PP), five had polyethylene (PE) spectral patterns and the remaining MP, represented by single particles, were made of polyvinyl chloride (PVC), polybutylene terephthalate (PBT), and silicone-based compounds (SI).

MP (> 11 µm) concentrations in precipitation and wet, dry and total deposition fluxes

MP concentrations in precipitation varied from 2 to 18 MP L^{-1} (Fig. 2a) and the precipitation weighted mean concentration was 7 ± 5 MP L^{-1} (mean ± SD). Thus, based on our samples, the estimated annual plastic wet deposition at the study site comprises approximately 4300 MP m^{-2} a^{-1}. Daily precipitation sums can be found in Fig. 1 and Online Resource ESM_1. Calculated mean wet, dry and total (wet + dry) DF (based on MP number) were 10 ± 5 MP m^{-2} day^{-1}, 7 ± 8 MP m^{-2} day^{-1}, and 17 ± 14 MP m^{-2} day^{-1}, respectively (Fig. 2b). The wet deposition from May to December was 59% of the total (wet + dry) MP atmospheric deposition.

The seasonal variation of dry deposition was similar to that of wet deposition. Among the wet/dry deposition measurements from May to December, the highest MP total DF were observed in August and September.

Correlations with meteorological variables

We investigated the relationship between wet, dry and total (wet + dry) DF and concentrations in precipitation, and meteorological variables by means of Spearman rank correlation analysis (Table 2).

MP dry DF did not correlate significantly with none of the studied meteorological parameters. Wet DF showed no significant correlations with most of the analysed parameters but showed a strong negative correlation with the maximum dry period (r_s = -0.96, $p = 0.0009$). MP concentrations in precipitation showed negative correlations with the precipitation amount (r_s = -0.78, $p = 0.02$) and average wet period (r_s = -0.87, $p = 0.005$), and positive correlation with the trajectory-averaged population density (r_s = 0.91, $p = 0.002$).

Although significant correlations were observed, correlation studies of MP DF/concentrations in precipitation with meteorological variables in our work should be used with

Table 1 MP particles detected in wet and dry atmospheric deposition samples using µFTIR down to 11 µm

Sample	MP detected in wet deposition, plastic type (length [µm], width [µm], colour)	MP detected in dry deposition, plastic type (length [µm], width [µm], colour)
May-19	PP (44, 22, w)	n. d.
Jun-19	PBT (11, 11, g); PP (60, 27, g)	n. d.
Jul-19	PP (34, 27, g)	n. d.
Aug-19	PP (22, 11, t); PE (130, 50, t); PP (111, 45, t)	PP (33, 22, g); PP (33, 33, t)
Sep-19	PE (22, 11, t); PE (56, 35, t); PP (27, 19, w)	PVC (11, 11, g); PP (66, 45, t); PP (44, 11, t)
Oct-19	PP (70, 43, g)	PP (45, 25, t)
Nov-19	PE (11, 11, g)	n. d.
Dec-19	PE (45, 45, g)	SI (46, 32, t)

n. d. – not detected, PP – polypropylene; PE – polyethylene; PBT – polybutylene terephthalate; PVC – polyvinyl chloride; SI – silicone-based compounds; w – white; g – grey; t – transparent

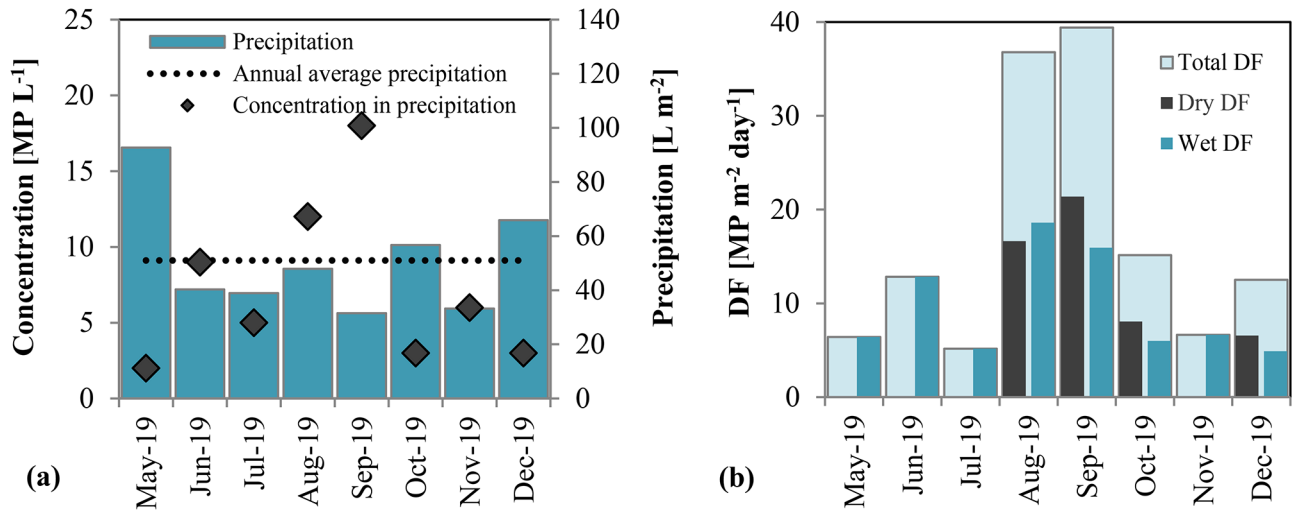

Fig. 2 Monthly variation in (**a**), MP concentrations in precipitation and total precipitation patterns at the study site during the sampling period, and (**b**) wet, dry, and total (wet + dry) atmospheric deposition of MP

Table 2 Correlation between meteorological variables and microplastic dry, wet, and total DF, and concentrations in precipitation*

Parameter	Dry DF [MP m^{-2} day^{-1}]	Wet DF [MP m^{-2} day^{-1}]	Total DF [MP m^{-2} day^{-1}]	C_{MP} [MP L^{-1}]
Average dry period [days]	-0.56	-0.21	-0.42	-0.12
Maximal dry period [days]	-0.40	**-0.96**	-0.61	-0.68
Average wet period [h]	-0.09	-0.58	-0.40	**-0.87**
Maximal wet period [h]	0.16	-0.28	-0.05	-0.58
Precipitation [mm]	0.29	-0.41	-0.20	**-0.78**
Light rain (drizzle, 0.2–0.5 mm h^{-1}) [h]	0.68	0.08	0.54	0.26
Moderate rain (0.5–4.0 mm h^{-1}) [h]	0.24	-0.02	-0.07	0.06
Heavy rain (4.0–24 mm h-1) [h]	-0.24	-0.17	-0.41	-0.58
Average rain intensity [mm h^{-1}]	-0.20	-0.14	-0.55	-0.39
Wind speed [m s^{-1}]	-0.04	-0.19	0.02	-0.55
Average wind direction [°]	0.19	-0.36	-0.29	-0.32
Trajectory-averaged population density [km^{-2}]	0.00	0.64	0.38	0.91
Temperature [°C]	0.17	0.09	0.03	0.34
Global radiation [W m^{-2}]	-0.31	0.04	-0.16	0.14
Air pressure [hPa]	-0.12	0.23	0.25	0.50
Relative humidity [%]	0.17	0.07	0.17	-0.09
PM10 [µg m^{-3}]	-0.23	-0.12	-0.35	0.06
SO_2 [µg m^{-3}]	-0.30	-0.48	-0.57	-0.16
NO [µg m^{-3}]	0.39	0.13	0.24	0.04
NO_2 [µg m^{-3}]	0.38	0.32	0.38	0.18
O_3 [µg m^{-3}]	-0.37	-0.20	-0.28	-0.07

*Spearman rank correlation coefficients between meteorological variables and MP DF and concentrations in precipitation: $p < 0.05$ (in bold), $p > 0.05$ (in regular font)

caution due to the fact that low numbers of MP particles were found in all samples and in 5 out of 8 dry deposition subsamples MP were not detected. For more reliable correlation analyses also more frequent sampling would be beneficial. However, the small number of particles identified by the method used in this study casts doubt on its usefulness.

Raman analysis

Exemplarily, one filter from the August dry deposition sample was selected and used for extensive Raman measurements to probe for plastic particles smaller than 11 µm in diameter. Wet deposition samples were in-situ filtered through a 10 µm stainless-steel filter and, thus, in-depth studies by Raman spectroscopy were not applicable. We scanned an Anodisc filter, which was also used for µFTIR analysis. No additional particle resuspension on a substrate more appropriate for Raman imaging was conducted. Low Raman background and flatness of the Anodisc filter, which is crucial for the narrow focal depth analyses, enabled further Raman imaging investigations (Zada et al. 2018). The sample areas randomly selected for extensive Raman measurements employing the WITec ParticleScout particle analysis tool and large area Raman mapping of an exemplarily dry deposition sample are displayed in Fig. 3a (area 1, 2 and 3a-c). In total, 1361 particles were found over the selected area 1, employing the WITec ParticleScout particle analysis tool of which 3 were assigned to plastics, i.e. polydimethylsiloxane (PDMS), PVC, and PP (Figs. 3b and 4). Thus, MP particles comprised 0.2% of all analysed particles in the 3×3 mm^2 screened area (see also Online Resource ESM_1). In comparison, scanning the entire particle loaded filter area

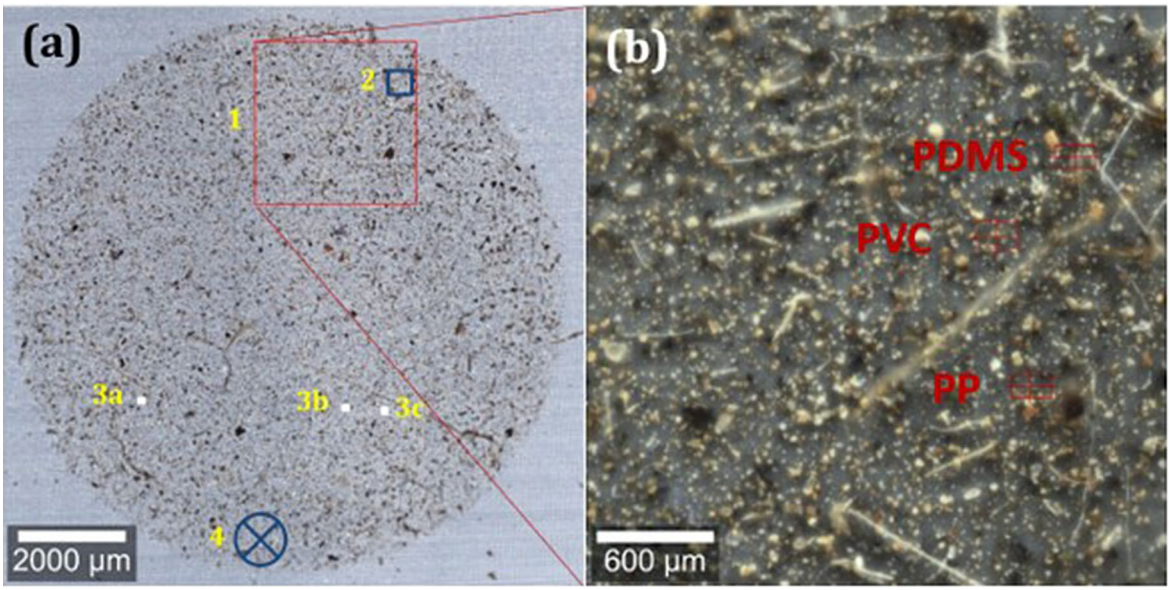

Fig. 3 (**a**) Optical microscopy stitching image of the selected filter showing the area 1 (red square 3 × 3 mm^2) employed for particle analysis with WITec ParticleScout, Raman imaging areas 2 (blue square 500 × 500 μm^2, employing integration time 0.8 s, step size 2 µm $pixel^{-1}$ and laser power 10 mW), and areas 3a-c (white squares 100 × 100 μm^2 each, employing integration time 0.6 s, step size 0.5 µm $pixel^{-1}$ and laser power 8 mW), and the location of the PP particle found by µFTIR (position 4, blue circle); (**b**) dark-field optical microscopy stitching image of area 1 in (a), being screened with WITec ParticleScout, and the position of detected MP particles

by using µFTIR, only one PP particle (Fig. 3a, position 4) was detected (see also Online Resource ESM_1).

Two identified particles made of PDMS (14 µm × 4 µm) and PP (9 µm × 9 µm) (Fig. 4a, c) fell in the size range where µFTIR is no longer applicable for reliable identification, but a slightly larger PVC particle (21 µm × 15 µm) (Fig. 4b) was likely overlooked by µFTIR. As suggested by Käppler et al. (2016) PVC particles seem better detectable by Raman spectroscopy compared to FTIR. This is potentially due to the characteristic relatively broad C–Cl stretching vibration at 690 cm^{-1}, which was not detectable due to the limited spectral range of the FPA detector (4000–900 cm^{-1}) in µFTIR in their study, or categorised as another chemical especially when containing high amounts of plasticisers (Käppler et al. 2016). Most of the other particles showed Raman spectra typical for inorganics i.e. black carbon (soot), quartz, titanium dioxide, and dolomite. Identified organic non-plastic particles were assigned to cellulose and bacteria (see Online Resource ESM_1).

Extrapolation of Raman results to the total effective filter surface (7.85×10^{-5} m^2), sampling surface (8.01×10^{-3} m^2) and collection time (35 days) gives a total dry DF of 207 MP per m^2 per day.

The large area Raman image with a step size of 2 µm $pixel^{-1}$ (Fig. 3a, area 2 (500 × 500 μm^2), enclosing the PDMS MP particle) is presented in Fig. 5. As shown in Fig. 5b (also Online Resource ESM_1), a large number of single particles in the lower micron range was detected. However, comparison of the particles' Raman spectra to the Raman spectra of the most common synthetic polymers did not result in a reliable particle assignment to plastics.

Moreover, large area Raman imaging with a step size of 0.5 µm $pixel^{-1}$ of three randomly selected 100 × 100 μm^2 quadrants did not result in plastic particle assignment in the submicron range (component distribution from Raman imaging and respective Raman spectra for one quadrant are given exemplarily in Online Resource ESM_1). Submicron-range particles made of quartz, calcite, soot, and most probably amylose or another polysaccharide were identified.

Discussion

Wet and dry microplastic deposition fluxes

Removal of particulate matter by dry and wet deposition is an important self-cleansing mechanism of the atmosphere (Jorgensen and Fath 2014). Gravitational settling, vertical turbulent motion, and surface conditions determine particle dry uptake at the Earth's surface (water, soil, vegetation, or buildings), whereas wet deposition processes refer to in-cloud and below-cloud scavenging, i.e., the uptake of pollutants into hydrometeors such as cloud and rain droplets, snowflakes, or hail (Hosker Jr and Lindberg 1982), and transport to the surface. The scavenging efficiency, i.e. the ratio of the concentration in precipitation to the total atmospheric concentration depends on particle size, particle

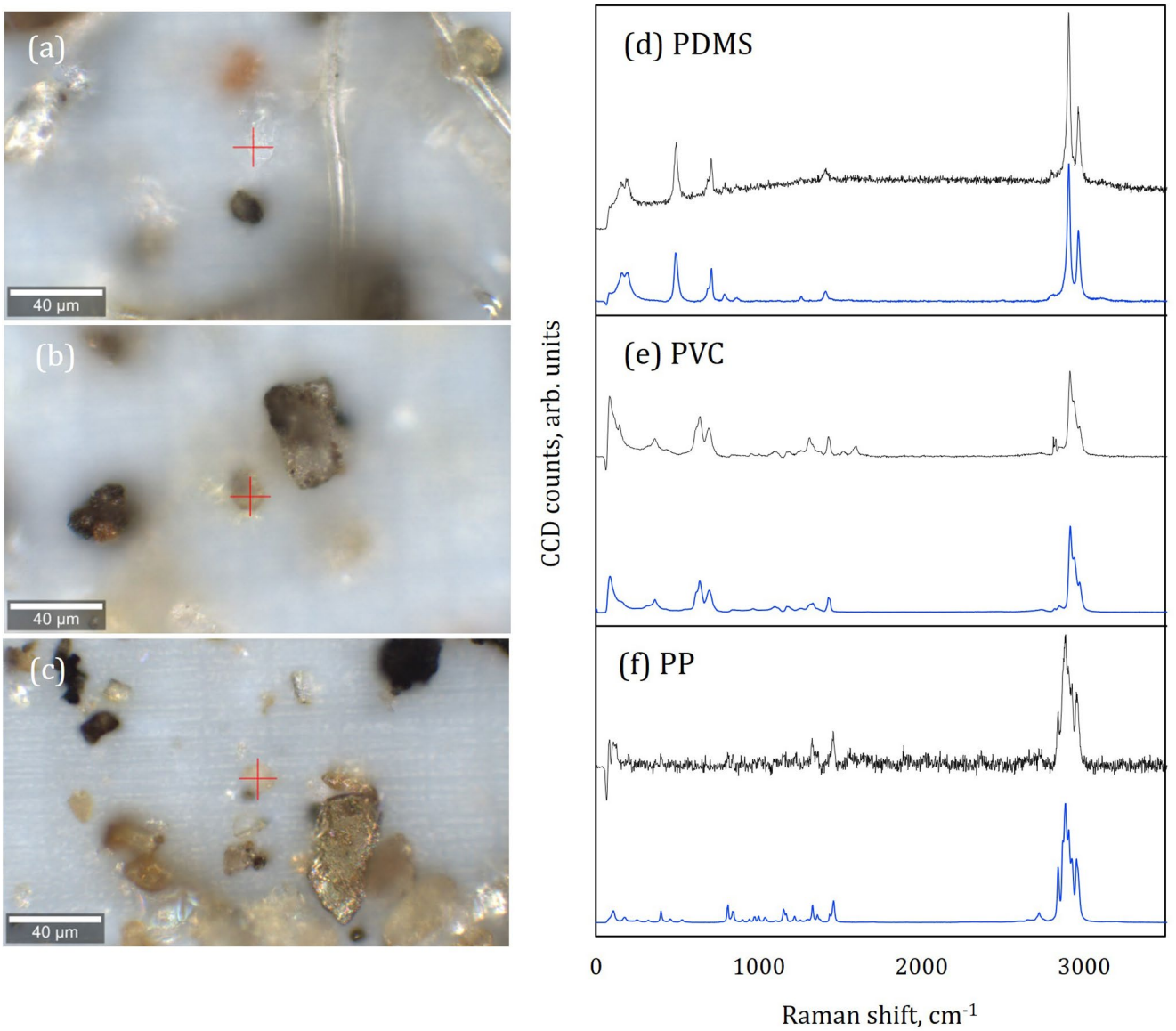

Fig. 4 Optical microscopy images of the detected (**a**) PDMS, (**b**) PVC, and (**c**) PP microplastic particles and (**d-f**) corresponding Raman spectra (black) compared to reference spectra from the database (blue)

composition, and precipitation type, amongst other factors (Cheng et al. 2021).

Dry DF can be expressed as a function of particle concentrations and size-dependent particle deposition velocities. Dry deposition of fine particles in the submicron and lower micron range is dominated by turbulence, which is affected by meteorological conditions near the surface, including wind speed, temperature, atmospheric stability and friction velocity, surface characteristics such as surface roughness, and particle properties such as particle size (Mariraj Mohan 2016). Coarse atmospheric particles in the diameter range larger than 10 µm mainly deposit by gravitational settling and impaction or interception (Droppo 2006). In contrast, the scavenging efficiency by wet deposition was found to be related to the duration and intensity of the precipitation event, as well as to the hydrometeor size distribution, the settling speed, the average collection efficiency, the shape of the hydrometeors and aerosol hydrophilicity (Jennings et al. 1998; Andronache 2004; Feng 2009). Moreover, Wu et al. (2018) found that removal of particles smaller than 2.5 µm by wet deposition to be more efficient than by dry deposition. Typically, wet deposition is considered easier to measure than dry deposition, and transferable to broad regions (Saylor et al. 2019; Farmer et al. 2021). Observational data of dry and wet DF of MP are required as input for simulating the MP deposition in global chemical transport and climate models.

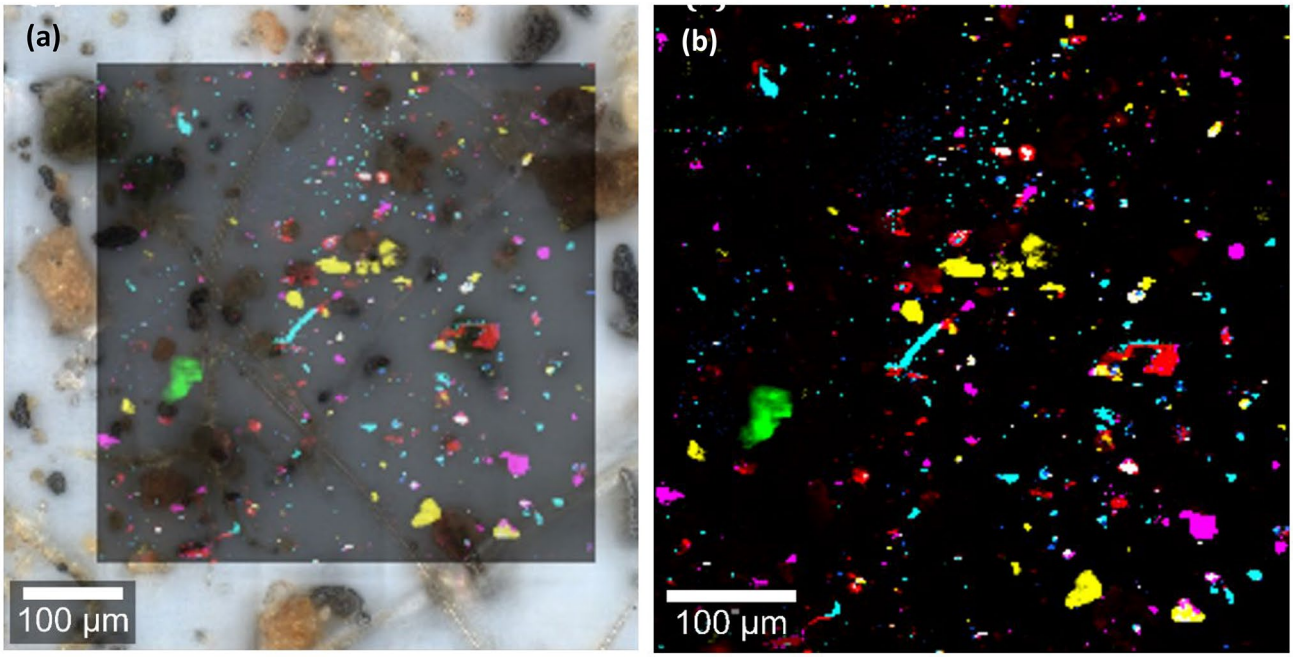

Fig. 5 (**a**) Overlay of optical microscopy image and component distribution from Raman imaging for the region where the PDMS MP particle was found; (**b**) component distribution from Raman imaging extracted by True Component Analysis, colour code corresponds to: red – carbon black, blue – titanium dioxide, green – PDMS MP particle, cyan – bacteria, purple – dolomite, and ochre – quartz. Raman spectra of the components are displayed in Online Resource ESM_1

So far, only a few studies have addressed microplastic separate atmospheric pathways and the impact of meteorology on MP deposition (Dris et al. 2016, 2017; Allen et al. 2019; Roblin et al. 2020; Brahney et al. 2020; Abbasi and Turner 2021). Dris et al. (2017) and Allen et al. (2019) showed that rain and snowfall play a significant role in MP scavenging from the atmosphere (Allen et al. 2019), resulting in a 5-fold increase in fibre deposition during rain events (Dris et al. 2017). Precipitation intensity was shown to contribute to MP deposition variability by up to two orders of magnitude (Dris et al. 2016). The wet-only deposition was estimated to capture ~70% of the bulk anthropogenic microfibre deposition in coastal areas around Ireland (Roblin et al. 2020). In contrast, more than 75% of the MP mass was removed from the atmosphere by dry depositin in US-protected areas (Brahney et al. 2020). Recently, Abbasi and Turner (2021) suggested that MP deposition in a semi-arid region of Iran was dominatedby dry deposition, while precipitation appeared to washout and inhibit local resuspension of MP by dampening the ground.

In this study, MP mean wet and dry DF derived from µFTIR measurements were 10 ± 5 MP m^{-2} day^{-1}, and 7 ± 8 MP m^{-2} day^{-1}, respectively. This indicates that both deposition modes are of similar importance at the study site and timeframe. The wet deposition was 59% of the total (wet + dry) MP number atmospheric deposition on average, and this value is in the range of the typical estimate of one-half of the total input of pollutant surface flux by wet deposition and the estimated loss of submicron particles by wet deposition of greater than 80% ued in atmospheric models (Emerson et al. 2020).

We investigated the relationship between dry and wet DF, concentrations in precipitation, and meteorological variables by means of Spearman rank correlation analysis (Table 2). MP dry DF did not correlate significantly with temperature, wind speed, relative humidity, and with none of the other studied meteorological parameters. Furthermore, wet DF did not show significant correlations with precipitation amount, intensity, or duration but showed a strong negative correlation with the maximal dry period, i.e. the longest continuous period without precipitation during sampling intervals. This points likely to low accumulation capability for MP particle > 11 µm in the atmosphere. Coarse MP particles tend to sediment faster and since no positive correlation between dry DF and maximal dry period was observed, MP sources might have local and temporally irregular emission patterns. MP concentrations in precipitation showed negative correlation with the precipitation amount and average wet period. This indicates dilution of precipitation samples and efficient MP scavenging by precipitation. It should be noted that more frequent sampling would make correlation measurements more reliable.

The wind rose plots for the study site and timeframe indicates that the prevailing wind direction was NE and SSW

(Fig. 1, see also Online Resource ESM_1). In May and July 2019, the dominant wind was blowing from the NE, and in the other months from the SSW. In months with prevailing SSW wind, we collected 90% of all detected MP particles in the total (wet + dry) deposition, 84% of all MP particles in wet deposition, and 100% of MP particles in dry deposition samples. The city centre of Kassel is situated SW of the sampling site; thus, the dominant SSW winds may provide the most probable vector for local MP pollution at the sampling site. Calculated deposition velocities of detected plastic particles in dry deposition samples ranged from 0.05 to 0.2 m s^{-1}, indicating relatively short-range transport phenomena. This supports the idea that MP pollution (> 11 µm) to the study site was brought from the nearest urban centre.

Since single-point local wind fields can be misleading and can differ from the regional wind conditions, air mass origin was also evaluated by calculating 24-hour back trajectories for the study site and sampling periods. Anthropogenic influence on MP DF may be estimated by averaging population densities along air mass back trajectories during each sampling period. MP concentrations in precipitation were higher when air masses arrived from more densely populated areas and correlated significantly with the trajectory-averaged population density (Table 2, see also Online Resource ESM_1). Thus, anthropogenic activities appear to contribute to airborne MP abundances.

Airborne microplastic sources

The sources and mechanisms of how MP particles enter the atmosphere are discussed in the scientific literature but are not fully understood. One of the most important sources of MP in the air are MP emissions from areas with high anthropogenic activities, households, and industrial objects. The likely sources of airborne MP fragments and films are abrasion from everyday plastic items (Allen et al. 2019). It has been shown that MP can be generated by simple activities in daily life, e.g. scissoring, tearing with hands, cutting with knives or twisting manually, to open plastics containers/bags/tapes/caps (Sobhani et al. 2020a). PE and PP are the leading polymers in Europe with the highest demand (PlasticsEurope 2020) and are mostly used in packaging, textiles and reusable products. The dominance of PP and PE particles in our samples and the significant correlation between MP concentrations in precipitation and trajectory-averaged population density confirm this and thus provide a reasonable and plausible source of MP in the air.

Airborne MP can be generated by abrasion of buildings, construction materials and released from plastic industry when producing, displacing or transporting plastic granulate and plastic incineration (Prata 2018; Can-Güven 2021). In our samples we found also MP particles made of PVC, PC, PBT and SI. PVC is used mainly in the production of pipes, profiles, resistant textiles, medical devices, and cable insulation (PlasticsEurope 2020). SI and PC are used in a wide variety of products, including automotive and transport applications, construction materials, medical devices, and food packaging. Silicone applications are found also in textile, leather and fibre industry (Andriot et al. 2007). PBT is mostly applied in the automotive, electronic and textile industry. Chain breakage, fragmentation in MP due to weathering and MP release from these plastic products can occur and thus be categorised as potential sources of MP in the air (Zhang et al. 2021; Shi et al. 2021; Chen et al. 2021). Automotive tire and road abrasion may contribute up to 93 vol% of traffic-related particulate matter near roads (Sommer et al. 2018). MP can be also lifted up into the air by wind erosion from urban surfaces (Abbasi et al. 2017), landfill sites and arable soils especially when spreading compost or sewage sludge on the fields (Mbachu et al. 2020). Recently, simulated laboratory experiments confirmed MP emission from soil surfaces via saltation (Bullard et al. 2020). Furthermore, MP may be emitted into the atmosphere from surface waters via impacting rain droplets (e.g. Lehmann et al. 2021), bubble bursting (Oehlschlägel et al. 2024) or jet ejection by wind and waves (Allen et al. 2020, 2022). Droplets ejected into the air by bubble bursting can contain a higher concentration of MP particles than the bulk water because MP particles may be enriched at the water-gas interface of rising bubbles (Oehlschlägel et al. 2024). Brahney et al. modelled the airborne MP contributions in the United States and reported re-emissions from road dust sources (84%), the ocean (11%) and agricultural field dust (Brahney et al. 2021). Abrasion of synthetic clothing during wearing, laundry and drying is believed to be the main source of airborne microfibres (Dris et al. 2016; Can-Güven 2021). As synthetic fibres were found in higher amounts in indoor air, MP fibres in outdoor air can result from mixing with indoor air (Dris et al. 2017).

We did not find any synthetic fibres in our samples, although our methodology does not exclude the detection of fibrous MP. Typically, the fibre dimensions are above 10 µm (Haghi et al. 2010; Wright et al. 2020) and would remain on the filters after sample processing. This indicates that fibres are not the dominant shape of MP at the study site. This observation is consistent with findings in three other studies conducted in the Weser river catchment (Germany) (Kernchen et al. 2021), in the Hamburg metropolitan area (Germany) (Klein and Fischer 2019), and in a remote, pristine mountain catchment (French Pyrenees) (France) (Allen et al. 2019), where 96.5%, 95% and 68% of all detected MP in the total deposition were in the shape of fragments. At the urban site in Humber region (UK) 67% of all identified MP particles in deposition samples were in shape of films and

24% were in shape of fragments (Jenner et al. 2022b). In comparison, more than 90% synthetic fibres were identified in total atmospheric deposition in London (UK) (Wright et al. 2020), Paris (France) (Dris et al. 2015), and Yantai city (China) (ZHOU et al. 2017), and fibres also predominated in atmospheric deposition samples from the Chinese cities of Dongguan (Cai et al. 2017) and Guangzhou (Huang et al. 2021), and in wet and dry deposition samples in remote conservation areas (United States) (Brahney et al. 2020). Our observations indicate that airborne MP have rather regional characteristics which is in agreement with other studies (Wright et al. 2020). MP abundance, shape and polymer type differ spatially and temporally, depending on the proximity of the airborne MP source and meteorology.

The emissions into the air and atmospheric transport of MP starts with the particle detachment from a substrate. Once in the air, MP can be transported over long distances by wind and eventually deposited back onto the Earth's surface closing so called plastic cycle. The atmospheric processes, e.g. the wind speed and directions, up/down drafts, convection lift and turbulence are considered as important vectors which affect MP transport, and which further influence the flux mechanism and fate of plastic pollution in both marine and terrestrial environments (Zhang et al. 2020).

Comparison with other studies

To enable comparability of MP deposition within this study and other studies, we calculated the mean total DF of MP by summing the wet and dry DF. The mean total DF determined in this study by µFTIR was 17 ± 14 MP m^{-2} day^{-1}. This value is comparable to DF in the urbanised coastal zone of the Gulf of Gdansk (Poland, 10 ± 8 MP m^{-2} day^{-1}) (Szewc et al. 2021), coastal areas in Ireland (12 MP m^{-2} day^{-1}) (Roblin et al. 2020) and in the city of Perpignan (France, 22 ± 14 MP m^{-2} day^{-1}) (Constant et al. 2020). The mean total MP DF we measured is slightly lower than mean MP DF in Dongguan city (China, 36 ± 7 MP m^{-2} day^{-1}) (Cai et al. 2017), and an order of magnitude lower than DF in Guangzhou (China, 114 ± 40 MP m^{-2} day^{-1}) (Huang et al. 2021), Paris (France, 118 MP m^{-2} day^{-1}) (Dris et al. 2015), remote conservation areas in US (132 MP m^{-2} day^{-1}) (Brahney et al. 2020), the metropolitan region of Hamburg (Germany, 275 MP m^{-2} day^{-1}) (Klein and Fischer 2019) and remote areas of the Pyrenees Mountains (France, 365 ± 69 MP m^{-2} day^{-1}) (Allen et al. 2019). The mean DF of non-fibrous MP-only in London (UK) was 59 ± 32 MP m^{-2} day^{-1} (Wright et al. 2020), which is in the same order of magnitude as in our study. Since 92% of all particles were in shape of fibres, the total MP deposition (all forms) in London was 771 ± 167 MP m^{-2} day^{-1}. In addition to the measurements at Phuoc Hiep Landfill (Vietnam, 1,356.8 MP m^{-2} day^{-1}) (Thinh et al. 2020), this is one of the highest MP DF reported in the current literature. The mean total MP DF found in this study is lower, but is of the same order of magnitude as MP total atmospheric deposition measurements at the site in 2018 (73 ± 21 MP m^{-2} day^{-1}) (Kernchen et al. 2021). However, the mean values of the two studies were derived from different experimental setups and refer to different sample months. It is important to note that differences in deposition fluxes between studies may also be due to different sample processing methods and analytical instrumentation.

µFTIR vs. Raman

It may be expected that MP particle numbers are underestimated by the sole application of µFTIR having a detection limit around 10 µm since several studies confirmed an increase in airborne MP particle numbers with decreasing particle size (Mbachu et al. 2020; Zhang et al. 2020). In this study, Raman spectroscopy was applied in order to gain insight into the abundance of dry deposited MP particles in the size range < 11 µm, i.e. particles which may enter the respiratory system via inhalation and may therefore affect human health (Anderson et al. 2012). The results of exemplary Raman analysis suggest that FTIR analysis compared to Raman analysis may lead to underestimation of MP DF by an order of magnitude; however, uncertainties due to the subsample analyses and extrapolation should be considered. Scanning a larger number of particles would give a more robust estimation of the dry DF. It was shown by other studies that FTIR imaging may lead to underestimation of MP number by about 35%, especially in the size range < 20 µm compared to Raman imaging (Käppler et al. 2016), and automated single-particle exploration coupled to µ-Raman (ASPEx-µ-Raman) quantified two-times higher MP numbers in the size range < 500 µm compared to FTIR imaging (Cabernard et al. 2018). This suggests that Raman analyses might typically yield higher deposition fluxes compared to FTIR imaging. Interesting fact is that submicron range MP were not detected in our study. If particles of the most common synthetic polymers would be present, the spectral assignment would be achieved (also in the submicron range). It is worth mentioning that only 0.04% of the sample area were scanned with a step size of 0.5 µm $pixel^{-1}$, and therefore, the analysed subsample is not representative. However, scanning only 1% of the filter area would require the analysis of 78 quadrants and > 500 h of instrumental time. With the applied spatially resolved detection of submicron particles it would take several days to scan a representative area of the sample. However, our filtration technique distributes the particles on the filter evenly, and if a vast amount of submicron plastic particles would be deposited on the sampling area, we would be able to detect at least

some of them. Our results suggest that atmospheric dry deposition samples do not contain a large number of fine plastic particles > 500 nm. This is consistent with the lowest deposition velocities of atmospheric particles in the so-called accumulation range from 100 nm to 1 µm (Seinfeld and Pandis 1998). Even if there is a large number of submicron MP particles in the atmosphere, reduced dry DF must be expected. Further Raman mapping analyses of aerosol samples collected by active pump sampling would give new insights into the abundance of airborne submicron plastic particles.

Conclusions and outlook

Dry and wet deposition processes of MP particles in the size > 11 µm were of similar range at a study site in Kassel, Central Germany. From May to December 2019, on average, wet removal mechanisms slightly dominated and comprised 59% of the total number deposition of MP particles. MP concentrations in precipitation correlated significantly with the population density along air mass trajectories. This indicates a direct anthropogenic influence on atmospheric MP concentrations, however, further studies correlating atmospheric MP concentrations and air mass origin are required to validate these findings and ultimately to better constrain atmospheric MP emission sources.

Use of µFTIR spectroscopy alone cannot reliably identify microplastics in atmospheric samples. MP DF derived from µFTIR analysis (diameter > 11 µm) and Raman analysis including smaller particles may differ by an order of magnitude or more. The DF calculated in our work using µFTIR are in the lower range of DF found in other studies but might be underestimated. Therefore, application of a combination of both µFTIR and Raman spectroscopy is recommended to estimate the atmospheric loads and deposition of plastics. Dry deposition of lower micron and submicron plastic particles was not observed to be significant in this study; however, further research is needed to assess the concentrations and the effects of fine MP particles in the atmosphere.

Supplementary Information The online version contains supplementary material available at https://doi.org/10.1007/s11869-024-01571-w.

Acknowledgements The authors would like to thank Agnes Bednorz for technical support. Many thanks to Dr. Franziska Luschtinetz (*KasselWasser*), for the collaboration and collection of the samples.

Author contributions All authors contributed to the research conception and design. Material preparation, data collection and analysis were performed by Sarmite Kernchen, Andrej Einhorn, Holger Schmalz, Martin G. J. Löder, and Christoph Georgi. The first draft of the manuscript was written by Sarmite Kernchen, and all authors commented on previous versions of the manuscript. All authors read and approved the final manuscript.

Funding The authors are grateful to BMBF and DFG for the financial support and for the support extension due to the Coronavirus crisis. The project was supported by the Federal Ministry of Education and Research (BMBF). Project funding ref. nr: 03F0789A, acronym PLAWES. Part of this work was funded by the Deutsche Forschungsgemeinschaft (DFG, German Research Foundation) – project nr. 391977956 – SFB1357.
Open Access funding enabled and organized by Projekt DEAL.

Data availability All data generated or analysed during this study are included in this published article and its supplementary information files.

Declarations

Ethics approval and consent to participate Not applicable.

Consent for publication Not applicable.

Competing interests The authors declare that they have no competing interests.

References

Abbasi S, Keshavarzi B, Moore F, Delshab H, Soltani N, Sorooshian A (2017) Investigation of microrubbers, microplastics and heavy metals in street dust: a study in Bushehr city. Iran Environ Earth Sci 76(23):798

Abbasi S, Turner A (2021) Dry and wet deposition of microplastics in a semi-arid region (Shiraz, Iran). Sci Total Environ 786:147358

Allen D, Allen S, Abbasi S, Baker A, Bergmann M, Brahney J, Butler T, Duce RA, Eckhardt S, Evangeliou N (2022) Microplastics and nanoplastics in the marine-atmosphere environment. Nat Reviews Earth Environ 3(6):393–405

Allen S, Allen D, Moss K, Le Roux G, Phoenix VR, Sonke JE (2020) Examination of the ocean as a source for atmospheric microplastics. PLoS ONE 15(5):e0232746

Allen S, Allen D, Phoenix VR, Le Roux G, JimÃ©nez PD, Simonneau A, Binet S, Galop D (2019) Atmospheric transport and deposition of microplastics in a remote mountain catchment. Nat Geosci 12(5):339–344

Amato-Lourenço LF, Carvalho-Oliveira R, Júnior GR, dos Santos Galvão L, Ando RA, Mauad T (2021) Presence of airborne microplastics in human lung tissue. J Hazard Mater:126124

Anbumani S, Kakkar P (2018) Ecotoxicological effects of microplastics on biota: a review. Environ Sci Pollut Res 25(15):14373–14396

Anderson JO, Thundiyil JG, Stolbach A (2012) Clearing the air: a review of the effects of particulate matter air pollution on human health. J Med Toxicol 8(2):166–175

Andriot M, Chao SH, Colas A, Cray SE, de Buyl F, DeGroot JV, Dupont A, Easton T, Garaud JL, Gerlach E (2007) Silicones in industrial applications. Inorg Polym:61–161

Andronache C (2004) Estimates of sulfate aerosol wet scavenging coefficient for locations in the Eastern United States. Atmos Environ 38(6):795–804

Bergmann M, Mützel S, Primpke S, Tekman MB, Trachsel J, Gerdts G (2019) White and wonderful? Microplastics prevail in snow from the Alps to the Arctic. Sci Adv 5(8):eaax1157

Brahney J, Hallerud M, Heim E, Hahnenberger M, Sukumaran S (2020) Plastic rain in protected areas of the United States. Science 368(6496):1257–1260

Brahney J, Mahowald N, Prank M, Cornwell G, Klimont Z, Matsui H, Prather KA (2021) Constraining the atmospheric limb of the plastic cycle. Signif Proc Natl Acad Sci. 118(16):e2020719118 https://doi.org/10.1073/pnas.2020719118

Bullard JE, Ockelford A, O'Brien P, Neuman CM (2020) Preferential transport of microplastics by wind. Atmos Environ 245:118038

Cabernard L, Roscher L, Lorenz C, Gerdts G, Primpke S (2018) Comparison of Raman and Fourier transform infrared spectroscopy for the quantification of microplastics in the aquatic environment. Environ Sci Technol 52(22):13279–13288

Cai L, Wang J, Peng J, Tan Z, Zhan Z, Tan X, Chen Q (2017) Characteristic of microplastics in the atmospheric fallout from Dongguan city, China: preliminary research and first evidence. Environ Sci Pollut Res 24(32):24928–24935

Can-Güven E (2021) Microplastics as emerging atmospheric pollutants: a review and bibliometric analysis. Air Qual Atmos Health 14(2):203–215

Cheng I, Al Mamun A, Zhang L (2021) A synthesis review on atmospheric wet deposition of particulate elements: scavenging ratios, solubility, and flux measurements. Environ Reviews 29(3):340–353

Chen Q, Wang Q, Zhang C, Zhang J, Dong Z, Xu Q (2021) Aging simulation of thin-film plastics in different environments to examine the formation of microplastic. Water Res 202:117462

Constant M, Ludwig W, Kerhervé P, Sola J, Charrière B, Sanchez-Vidal A, Canals M, Heussner S (2020) Microplastic fluxes in a large and a small Mediterranean river catchments: the Têt and the Rhône, Northwestern Mediterranean Sea. Sci Total Environ 716:136984

Dietze V, Fricker M, Goltzsche M, Schultz E (2006) Air quality measurement in German health resorts-part 1: methodology and verification. GEFAHRSTOFFE Reinhalt DER LUFT-GERMAN Ed 66(1/2):45

Dris R, Gasperi J, Mirande C, Mandin C, Guerrouache M, Langlois V, Tassin B (2017) A first overview of textile fibers, including microplastics, in indoor and outdoor environments. Environ Pollut 221:453–458

Dris R, Gasperi J, Rocher V, Saad M, Renault N, Tassin B (2015) Microplastic contamination in an urban area: a case study in Greater Paris. Environ Chem 12(5):592–599

Dris R, Gasperi J, Saad M, Mirande C, Tassin B (2016) Synthetic fibers in atmospheric fallout: a source of microplastics in the environment? Mar Pollut Bull 104(1–2):290–293

Droppo JG (2006) Improved formulations for air-surface exchanges related to National Security needs. dry deposition models

Emerson EW, Hodshire AL, DeBolt HM, Bilsback KR, Pierce JR, McMeeking GR, Farmer DK (2020) Revisiting particle dry deposition and its role in radiative effect estimates. Proceedings of the National Academy of Sciences 117(42):26076–26082

Enyoh CE, Verla AW, Verla EN, Ibe FC, Amaobi CE (2019) Airborne microplastics: a review study on method for analysis, occurrence, movement and risks. Environ Monit Assess 191(11):668

Fang M, Liao Z, Ji X, Zhu X, Wang Z, Lu C, Shi C, Chen Z, Ge L, Zhang M (2022) Microplastic ingestion from atmospheric deposition during dining/drinking activities. J Hazard Mater 432:128674

Farmer DK, Boedicker EK, DeBolt HM (2021) Dry deposition of atmospheric aerosols: approaches, observations, and mechanisms. Annu Rev Phys Chem 72:375–397

Feng J (2009) A size-resolved model for below-cloud scavenging of aerosols by snowfall. J Geophys Research: Atmos 114(D8)

González-Pleiter M, Edo C, Aguilera Á, Viúdez-Moreiras D, Pulido-Reyes G, González-Toril E, Osuna S, de Diego-Castilla G, Leganés F, Fernández-Piñas F (2021) Occurrence and transport of microplastics sampled within and above the planetary boundary layer. Sci Total Environ 761:143213

Goodman KE, Hare JT, Khamis ZI, Hua T, Sang Q-XA (2021) Exposure of human lung cells to Polystyrene Microplastics significantly retards cell proliferation and triggers morphological changes. Chem Res Toxicol 34(4):1069–1081

Haghi AK, Aslp KH, Sabermaash E (2010) A review on electrospun polymeric nanosized fibres. J Balkan Tribological Association 16(4):570–584

Hartmann NB, Huffer T, Thompson RC, Hassellöv M, Verschoor A, Daugaard AE, Rist S, Karlsson T, Brennholt N, Cole M (2019) Are we speaking the same language? Recommendations for a definition and categorization framework for plastic debris

Horton AA, Cross RK, Read DS, Jürgens MD, Ball HL, Svendsen C, Vollertsen J, Johnson AC (2021) Semi-automated analysis of microplastics in complex wastewater samples. Environ Pollut 268:115841

Hosker RP Jr, Lindberg SE (1982) Atmospheric deposition and plant assimilation of gases and particles. Atmospheric Environment (1967) 16(5):889–910

Huang Y, He T, Yan M, Yang L, Gong H, Wang W, Qing X, Wang J (2021) Atmospheric transport and deposition of microplastics in a subtropical urban environment. J Hazard Mater:126168

Huang Y, Qing X, Wang W, Han G, Wang J (2020) Mini-review on current studies of airborne microplastics: Analytical methods, occurrence, sources, fate and potential risk to human beings. TRAC Trends Anal Chem 125:115821

Hufnagl B, Steiner D, Renner E, Löder MGJ, Laforsch C, Lohninger H (2019) A methodology for the fast identification and monitoring of microplastics in environmental samples using random decision forest classifiers. Anal Methods 11(17):2277–2285

Hufnagl B, Stibi M, Martirosyan H, Wilczek U, Möller JN, Löder MGJ, Laforsch C, Lohninger H (2021) Computer-assisted analysis of Microplastics in Environmental samples based on μFTIR Imaging in Combination with Machine Learning. Environ Sci Technol Lett 9(1):90–95

Jenner LC, Rotchell JM, Bennett RT, Cowen M, Tentzeris V, Sadofsky LR (2022a) Detection of microplastics in human lung tissue using μFTIR spectroscopy. Science of the Total Environment:154907

Jenner LC, Sadofsky LR, Danopoulos E, Chapman E, White D, Jenkins RL, Rotchell JM (2022b) Outdoor Atmospheric Microplastics within the Humber Region (United Kingdom): quantification and chemical characterisation of deposited particles Present. Atmosphere 13(2):265

Jennings SG, Harrison RM, van Grieken R (1998) Wet processes affecting atmospheric aerosols. Atmospheric Particles:475–508

Jorgensen SE, Fath BD (2014) Encyclopedia of ecology. Newnes

Kalnay E, Kanamitsu M, Kistler R, Collins W, Deaven D, Gandin L, Iredell M, Saha S, White G, Woollen J (1996) The NCEP/NCAR 40-year reanalysis project. Bull Am Meteorol Soc 77(3):437–472

Kernchen S, Löder MGJ, Fischer F, Fischer D, Moses SR, Georgi C, Nölscher AC, Held A, Laforsch C (2021) Airborne microplastic

concentrations and deposition across the Weser River catchment. Science of the Total Environment:151812
Klein M, Fischer EK (2019) Microplastic abundance in atmospheric deposition within the Metropolitan area of Hamburg, Germany. Sci Total Environ 685:96–103
Käppler A, Fischer D, Oberbeckmann S, Schernewski G, Labrenz M, Eichhorn K-J, Voit B (2016) Analysis of environmental microplastics by vibrational microspectroscopy: FTIR, Raman or both? Analytical and bioanalytical chemistry 408(29):8377–8391
Löder MGJ, Kuczera M, Mintenig S, Lorenz C, Gerdts G (2015) Focal plane array detector-based micro-fourier-transform infrared imaging for the analysis of microplastics in environmental samples. Environ Chem 12(5):563–581
Lehmann M, Oehlschlägel LM, Häusl FP, Held A, Gekle S (2021) Ejection of marine microplastics by raindrops: a computational and experimental study. Microplastics Nanoplastics 1(1):1–19
Levermore JM, Smith TEL, Kelly FJ, Wright SL (2020) Detection of microplastics in ambient particulate matter using Raman spectral imaging and chemometric analysis. Anal Chem 92(13):8732–8740
Manisalidis I, Stavropoulou E, Stavropoulos A, Bezirtzoglou E (2020) Environmental and health impacts of air pollution: a review. Front Public Health 8:14
Mariraj Mohan S (2016) An overview of particulate dry deposition: measuring methods, deposition velocity and controlling factors. Int J Environ Sci Technol 13(1):387–402
Mbachu O, Jenkins G, Pratt C, Kaparaju P (2020) A new contaminant superhighway? A review of sources, measurement techniques and fate of atmospheric microplastics. Water Air Soil Pollut 231(2):1–27
Oehlschlägel LM, Schmid S, Lehmann M, Gekle S, Held A (2024) Water–air transfer rates of microplastic particles through bubble bursting as a function of particle size. Microplastics Nanoplastics 4(1):1
PlasticsEurope (2020), Plastics - the Facts 2020.
Prata JC (2018) Airborne microplastics: consequences to human health? Environ Pollut 234:115–126
Revell LE, Kuma P, Le Ru EC, Somerville WRC, Gaw S (2021) Direct radiative effects of airborne microplastics. Nature 598(7881):462–467
Roblin B, Ryan M, Vreugdenhil A, Aherne J (2020) Ambient Atmospheric Deposition of Anthropogenic Microfibers and microplastics on the western periphery of Europe (Ireland). Environ Sci Technol 54(18):11100–11108
Saylor RD, Baker BD, Lee P, Tong D, Pan L, Hicks BB (2019) The particle dry deposition component of total deposition from air quality models: right, wrong or uncertain? Tellus B: Chem Phys Meteorol 71(1):1550324
Schwaferts C, Niessner R, Elsner M, Ivleva NP (2019) Methods for the analysis of submicrometer-and nanoplastic particles in the environment. TRAC Trends Anal Chem 112:52–65
Schymanski D, Oßmann BE, Benismail N, Boukerma K, Dallmann G, Esch E, von der, Fischer D, Fischer F, Gilliland D, Glas K (2021) Analysis of microplastics in drinking water and other clean water samples with micro-raman and micro-infrared spectroscopy: minimum requirements and best practice guidelines. Anal Bioanal Chem 413(24):5969–5994
Seinfeld JH, Pandis SN (1998) Atmospheric Chemistry and Physics: from air pollution to climate change. John Willey & Sons, New York
Shaddick G, Thomas ML, Mudu P, Ruggeri G, Gumy S (2020) Half the world's population are exposed to increasing air pollution. NPJ Clim Atmospheric Sci 3(1):1–5
Shi Y, Liu P, Wu X, Shi H, Huang H, Wang H, Gao S (2021) Insight into chain scission and release profiles from photodegradation of polycarbonate microplastics. Water Res 195:116980
Sobhani Z, Lei Y, Tang Y, Wu L, Zhang X, Naidu R, Megharaj M, Fang C (2020a) Microplastics generated when opening plastic packaging. Sci Rep 10(1):1–7
Sobhani Z, Zhang X, Gibson C, Naidu R, Megharaj M, Fang C (2020b) Identification and visualisation of microplastics/nanoplastics by Raman imaging (i): down to 100 nm. Water Res 174:115658
Sommer F, Dietze V, Baum A, Sauer J, Gilge S, Maschowski C, Gieré R (2018) Tire abrasion as a major source of microplastics in the environment. Aerosol Air Qual Res 18(8) 2014–2028 https://doi.org/10.4209/aaqr.2018.03.0099
Stein AF, Draxler RR, Rolph GD, Stunder BJB, Cohen MD, Ngan F (2015) NOAA's HYSPLIT atmospheric transport and dispersion modeling system. Bull Am Meteorol Soc 96(12):2059–2077
Szewc K, Graca B, Dołęga A (2021) Atmospheric deposition of microplastics in the coastal zone: characteristics and relationship with meteorological factors. Sci Total Environ 761:143272
Thinh TQ, Sang TTN, Viet TQ, Dan NP, Strady E, Le Chung KT (2020) Preliminary assessment on the microplastic contamination in the atmospheric fallout in the Phuoc Hiep landfill, Cu Chi, Ho Chi Minh city. Vietnam J Sci Technol Eng 62(3):83–89
Trainic M, Flores JM, Pinkas I, Pedrotti ML, Lombard F, Bourdin G, Gorsky G, Boss E, Rudich Y, Vardi A (2020) Airborne microplastic particles detected in the remote marine atmosphere. Commun Earth Environ 1(1):1–9
VDI2119 (2013) Ambient air measurements sampling of atmospheric particles > 2.5 µm on an acceptor surface using the Sigma-2 passive sampler, characterization by optical microscopy and calculation of number settling rate and mass concentration. 13.040.01, vol ICS. Beuth, Berlin
Waza A, Schneiders K, May J, Rodríguez S, Epple B, Kandler K (2019) Field comparison of dry deposition samplers for collection of atmospheric mineral dust: results from single-particle characterization. Atmos Meas Tech 12(12):6647–6665
Wright SL, Ulke J, Font A, Chan KL, Kelly FJ (2020) Atmospheric microplastic deposition in an urban environment and an evaluation of transport. Environ Int 136:105411
Wu Y, Liu J, Zhai J, Cong L, Wang Y, Ma W, Zhang Z, Li C (2018) Comparison of dry and wet deposition of particulate matter in near-surface waters during summer. PLoS ONE 13(6):e0199241
Zada L, Leslie HA, Vethaak AD, Tinnevelt GH, Jansen JJ, de Boer JF, Ariese F (2018) Fast microplastics identification with stimulated Raman scattering microscopy. J Raman Spectrosc 49(7):1136–1144
Zhang K, Hamidian AH, Tubić A, Zhang Y, Fang JKH, Wu C, Lam PKS (2021) Understanding plastic degradation and microplastic formation in the environment: a review. Environ Pollut 274:116554
Zhang S, Wang J, Liu X, Qu F, Wang X, Wang X, Li Y, Sun Y (2019) Microplastics in the environment: a review of analytical methods, distribution, and biological effects. TRAC Trends Anal Chem 111:62–72
Zhang Y, Kang S, Allen S, Allen D, Gao T, Sillanpää M (2020) Atmospheric microplastics: a review on current status and perspectives. Earth Sci Rev 203:103118
ZHOU Q, TIAN C, LUO Y (2017) Various forms and deposition fluxes of microplastics identified in the coastal urban atmosphere. Chin Sci Bull 62(33):3902–3909